ELSEVIER

Biophysical Chemistry 55 (1995) 185–196

Biophysical Chemistry

Review

Cyclic nucleotide-gated channels in visual and olfactory transduction ☆

Anna Menini *

Istituto di Cibernetica e Biofisica, Consiglio Nazionale delle Ricerche, Via de Marini 6, 16149 Genova, Italy

Received 15 May 1994; revised 29 November 1994; accepted 2 December 1994

Abstract

Rod and cone photoreceptors are the light detectors in the visual system whereas olfactory receptor cells are the odorant detectors in the olfactory system. Despite the two very different types of stimuli, light in photoreceptors, and odorant molecules in olfactory receptor cells, the mechanisms of visual and olfactory transduction appear to have many homologies. Both stimuli trigger a chain of enzymatic events that terminates in a change in the concentration of a cyclic nucleotide: a decrease in the concentration of cGMP in photoreceptors, and an increase in the concentration of cAMP in olfactory receptor cells. These cyclic nucleotides directly gate cation channels and therefore a change in their concentration induced by the external stimulus is converted into an electrical signal. The analysis of the ionic selectivity properties of cyclic nucleotide-gated channels in retinal rods, cones and in olfactory receptor cells shows that there are many similarities between these channels. They do not appreciably select between alkali monovalent cations and can be permeated and blocked by divalent cations. Their ionic permeation properties are consistent with the presence of a cation-binding site of high-field strength in the pore.

Keywords: Visual transduction; Olfactory transduction; Ion channel; Cyclic nucleotide

Contents

☆ This article is based on the presentation given at the 11th International Biophysics Congress, July 25–30, 1993, Budapest, Hungary.

* Corresponding author.

SSDI 0301-4622(94)00153-7

1. Visual and olfactory transduction: electrical properties and biochemical schemes

The initial steps of vision and olfaction occur in sensory receptor cells devoted to convert external stimuli into electrical signals that will be transmitted to other neurons. Although these two sensory modalities deal with very different stimuli, they use some similar mechanisms of signal transduction.

Visual transduction in vertebrate photoreceptors, rods or cones, is initiated by the absorption of a photon by a visual pigment protein. Rhodopsin is the rod pigment and mediates vision in dim light, whereas the blue, green and red pigments of the cones mediate color vision. The absorption of a photon triggers an enzymatic cascade that causes the closure of ion channels, reducing an inward current carried by Na and Ca and causing membrane hyperpolarization. Light of increasing intensity gradually suppresses the current flowing in the dark as shown in Fig. 1 [1].

Similarly olfactory transduction is initiated by the interaction of odors with receptors on olfactory receptor cells. The binding of odorant molecules triggers an enzymatic cascade that leads to the onset of an ionic current and depolarization of the membrane. In photoreceptors there are only four visual pigment proteins able to capture light whereas in olfactory receptor cells there is a very large family of receptors able to bind different odorants. A family of current responses obtained by exposing an olfactory receptor cell to increasing odorant concentrations is shown in Fig. 2 [2]. Contrary to the case of visual transduction application of odorants of increasing concentration gradually induced larger currents.

By comparing Figs. 1 and 2 it is evident that the kinetics of the odorant-induced current has a time course broadly resembling the time course of the light-suppressed current and it is not surprising that the transduction mechanism in olfactory neurons and in photoreceptors is controlled by a similar enzymatic cascade [3]. Both visual and olfactory transduction involve the activation of receptor molecules by the stimulus, which is followed by G protein-mediated enzymatic cascades leading to a change in the intracellular concentration of a second messenger: a cyclic nucleotide. In photoreceptors light causes the activation of phosphodiesterase that reduces the cGMP concentration from its resting level of some micromolar. In olfactory receptor cells odorants produce the activation of adenylate cyclase that increases the cAMP concentration. Cyclic nucleotides directly gate ion channels in the plasma

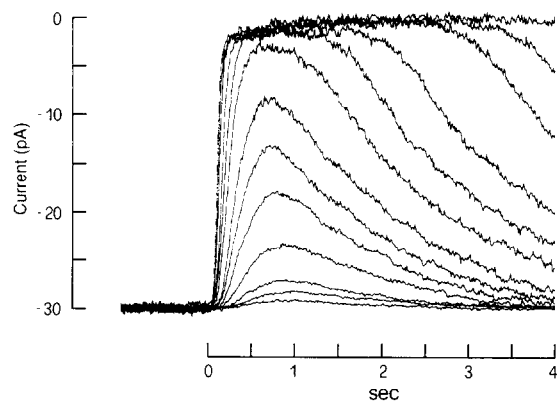

Fig. 1. Family of current responses to flashes of light of increasing intensity recorded from an isolated retinal rod of the newt. Brief flashes were given at time zero. Reproduced from Ref. [1].

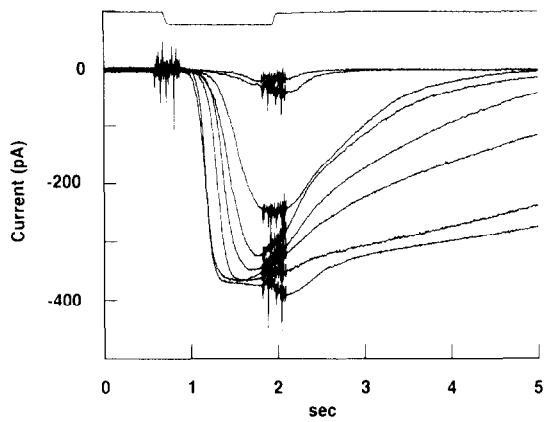

Fig. 2. Family of current responses to different concentrations of the odorant acetophenone, recorded from an isolated olfactory receptor cell of the salamander. The top trace represents the stimulus time course. Modified from Ref. [2].

membrane of these sensory cells: cGMP is the intracellular messenger involved in visual transduction whereas cAMP is involved in olfactory transduction. The modulation of the cyclic nucleotide concentration generates the electrical response in both visual and olfactory transduction pathways (see Refs. [4–6] for reviews on visual transduction and Refs. [7,8] for reviews on olfactory transduction).

The transduction process in photoreceptors is at the moment the best understood and it has been possible to make models [1,9,10] describing the measured electrophysiological properties of isolated photoreceptors on the basis of the known biochemistry of the transduction process. It will be very interesting to develop similar models also for the olfactory receptor cells, but in order to do so we still need some information on the biochemical steps of the transduction process and on the electrophysiological properties of isolated olfactory receptor cells.

2. Gating by cyclic nucleotides

2.1. Hill equation

Fesenko et al. [11] first showed that cGMP directly opens channels in excised membrane patches from retinal rod outer segments and similar channels were also described in retinal cones [12]. In 1987 Nakamura and Gold [13] first measured a conductance activated by cyclic nucleotides in the plasma membrane of cilia from olfactory receptor neurons. The opening of these channels is probably caused by a conformational change in the channel protein after the direct binding of several cyclic nucleotide molecules.

Cyclic nucleotide-gated channels in excised membrane patches from photoreceptors and olfactory receptor neurons can be activated both by cGMP and by cAMP but with very different affinities (see Table 1). Photoreceptor channels are usually called cGMP-gated channels because cGMP is the second messenger in visual transduction whereas olfactory channels are usually called cAMP-gated channels because cAMP is involved in olfactory transduction.

The ligand specificity of the conductance is determined by measuring the current as a function of the concentration of different cyclic nucleotides. The relation between activated current and cyclic nucleotide concentration is described by the Hill equation:

$$I = I_{max} c^n / \left(c^n + K_{1/2}^n \right) \quad (1)$$

Table 1
Properties of cyclic nucleotide-gated channels

	Retinal rod	Retinal cone	Olfactory receptor cell
$K_{1/2}$(cGMP)	9.8 μM	42 μM	1.5 μM
$K_{1/2}$(cAMP)	846 μM		4.0 μM
$I_{max(cAMP)}/I_{max(cGMP)}$	0.4		1
n(cGMP)	2.2	2.5	1.4
n(cAMP)	1.8		1.6

A comparison of the parameters of the Hill Eq. (1) for cyclic nucleotide-activated channels from retinal rod of the salamander [18], retinal cone of the striped bass [20] and olfactory receptor cell of the frog [22].

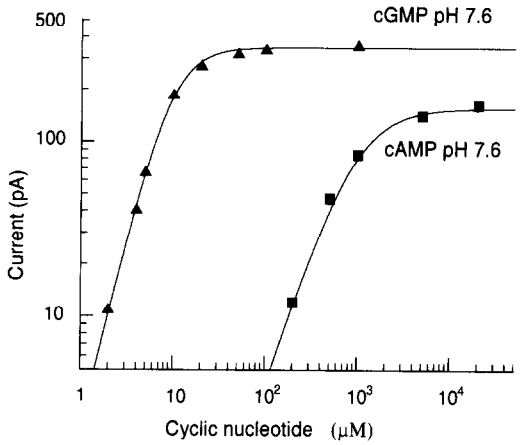

Fig. 3. Current measured at +60 mV as a function of different concentrations of cGMP or cAMP in an inside-out excised patch from a retinal rod outer segment of the salamander. The continuous lines are the best fit of the Hill Eq. (1) to the data with the following values: I_{max}(cGMP) = 365 pA, $K_{1/2}$(cGMP) = 9.8 μM, n(cGMP) = 2.2, I_{max}(cAMP) = 152 pA, $K_{1/2}$(cAMP) = 846 μM, n(cAMP) = 1.8. Unpublished results of A. Menini et al. [18].

where I is the activated current, I_{max} the maximal current, c the cyclic nucleotide concentration, $K_{1/2}$ the cyclic nucleotide concentration activating half of the maximal current and n is the Hill coefficient.

Half maximal activation of the rod channels occurs at cGMP concentrations between 10 and 50 μM [11,14–18] depending on animal species. The rod channels can also be activated by cAMP, but the half maximal concentration for activation by this cyclic nucleotide is much higher. In the salamander $K_{1/2}$ for cGMP is about 10 μM whereas $K_{1/2}$ for cAMP is about 850 μM, and the maximal current activated by cAMP is only 40% of that activated by cGMP [18] (see Fig. 3 and Table 1). The cone channels are half-activated at a cGMP concentration around 30–50 μM [19,20]. Channels of olfactory receptor cells are activated by lower cyclic nucleotide concentrations: between 2 and 22 μM for cAMP and between 1 and 4 μM for cGMP [13,21–23], depending on the species.

Activation by cyclic nucleotides shows a clear cooperativity. The Hill coefficient in Eq. (1) ranges between 1.2 and 3.1 for cyclic nucleotide-gated channels from both photoreceptor [11,14–20] and olfactory receptor cells [13,21–23] suggesting that the opening of a single channel depends on the cooperative binding of at least three cyclic nucleotide molecules.

2.2. Modulation of ligand sensitivity

The sensitivity of these channels for cyclic nucleotides can be modulated by several mechanisms. Gordon et al. [24] have shown that the channel in retinal rod can be converted between low and high sensitivity states with a variation of $K_{1/2}$ for cGMP of almost 10-fold and that this process is controlled by phosphorylation. They suggest that there are two phosphorylation sites on the channel and/or associated regulatory protein(s) that could modulate the sensitivity of the channel to cGMP in a reciprocal manner. Calmodulin also influences the activation by cyclic nucleotides of both the retinal rod and the olfactory receptor cell channels. The addition of calmodulin and Ca produces an increase of the $K_{1/2}$ for cGMP of 2-fold for the retinal rod channel [25] and an increase of the $K_{1/2}$ for cAMP of up to 20-fold for the olfactory channel [26].

pH also modulates the sensitivity of the retinal rod channel for cAMP [18,27], as described in Section 3.4.

3. Ionic selectivity and blockage

3.1. Alkali monovalent cations

Cyclic nucleotide-gated channels from retinal rod, cone and olfactory receptor cells have similar selectivity properties. These channels are cation selective and do not appreciably select between different alkali monovalent cations [16,20,22,28,29].

Fig. 4A shows currents activated by 100 μM cGMP in excised patches from retinal rods when the extracellular side of the patch was bathed with 110 mM NaCl and the cytoplasmic side was bathed in 110 mM NaCl, LiCl, KCl, RbCl or CsCl, in the absence of divalent cations. Fig. 4B shows the I–V relations obtained from the experiment illustrated in A [28].

Permeability ratios were calculated with the Goldman–Hodgkin–Katz potential equation (Eq. 2) from the measured reversal potentials. When the only permeant cation present at the external side of the

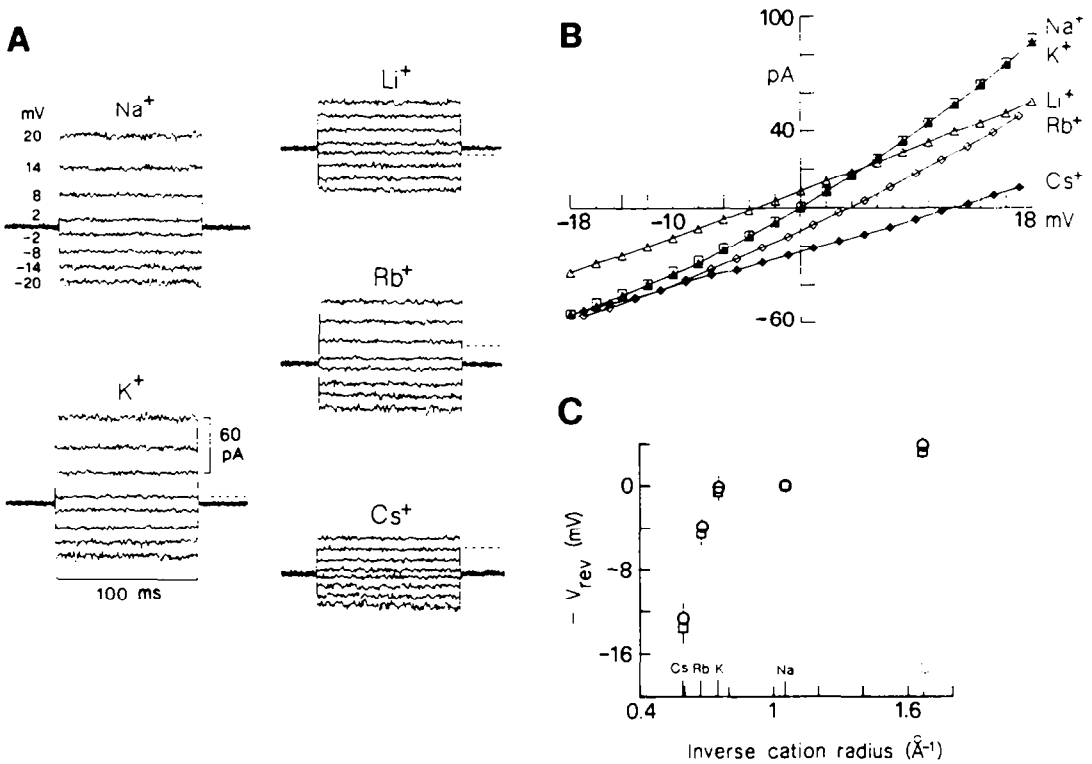

Fig. 4. (A) Currents activated by 100 μM cGMP in a patch excised from a retinal rod outer segment of the salamander. The solution filling the patch pipette contained 110 mM NaCl, whereas the solution at the cytoplasmic side of the patch contained 110 mM NaCl, KCl, LiCl, RbCl or CsCl, in the absence of divalent cations. Voltage pulses increasing and decreasing in steps of 2 mV were given from a holding potential of 0 mV. Each trace was obtained by subtraction of records in the presence and in the absence of cGMP. The dashed lines indicate the zero-current level. (B) Current–voltage relations corrected for junction potentials from the results of the experiments shown in (A). (C) Reversal potentials plotted as a function of the inverse of the Pauling radius for alkali cations. Reproduced from Ref. [28].

membrane patch is Na and the only permeant cation present at the intracellular side is X, the permeability ratio is:

$$P_X/P_{Na} = ([Na]_o/[X]_i)\exp(-FV_{rev}/RT) \qquad (2)$$

where R is the gas constant, F the Faraday constant, T the absolute temperature, $[Na]_o$ the Na concentration at the extracellular side and $[X]_i$ the concentration of the cation X at the cytoplasmic side of the membrane.

The ionic selectivity measured as permeability ratios, for cGMP-gated channels from retinal rods [28], cones [20], and for cAMP-gated channels from olfactory receptor cells [22] is shown in Table 2. It is evident that these cyclic nucleotide-activated channels poorly discriminate between alkali cations.

Eisenman (see for a review Ref. [30]) formulated an electrostatic model for selectivity among alkali monovalent cations based on the balance between the energy of dehydration of the cation and the energy of interaction with a binding site and predicted eleven cation selectivity sequences for the five alkali metal cations. The different selectivity se-

Table 2
Permeability ratios for alkali cations in cyclic nucleotide-gated channels

	Li	Na	K	Rb	Cs
Retinal rod	1.14	1	0.98	0.84	0.58
Retinal cone	0.99	1	1.11	0.96	0.80
Olfactory receptor cell	0.74	1	0.81	0.60	0.52

Permeability ratios relative to Na, P_X/P_{Na}, calculated with the GHK Eq. (2) for the cGMP-gated channel of retinal rod from the salamander [28], the cGMP-gated channel of retinal cone of the striped bass [20], and for the cAMP-gated channel of olfactory receptor cell of the frog [22].

quences are caused by variations of the field strength of the site. The permeability sequence of the rod channel corresponds to Eisenman sequence XI [28], that of the olfactory channel to sequence IX [22], and that of the cone channel is also similar to sequence IX [20], indicating that cations interact with strong-field-strength sites within the pore during the permeation process.

A useful model for describing the permeation of ions through channels is the rate-theory or Eyring barrier model. In this model the channel is represented by an energy profile, having maxima (barriers) and minima (wells or binding sites), encountered by an ion crossing the channel. Ions must move in single file and bind to sites inside the pore during the permeation process. Channels are often divided in two main categories: one-ion or multi-ion channels, depending on how many ions they may accommodate in their inner pore at a time. One-ion channels may also have several internal binding sites, but only one ion can be present in the pore at a time. One-ion channels are characterized by the following properties: (1) the permeability ratios among different ions are constant, independent of ion activity; (2) the dependence of the current on the activity of the permeating ion is a simple saturating function described by the Michaelis–Menten equation; and (3) the current and the reversal potential are monotonic functions of mole fraction when measured in mixtures of two permeating ions (see Ref. [31] for a review of permeability theories).

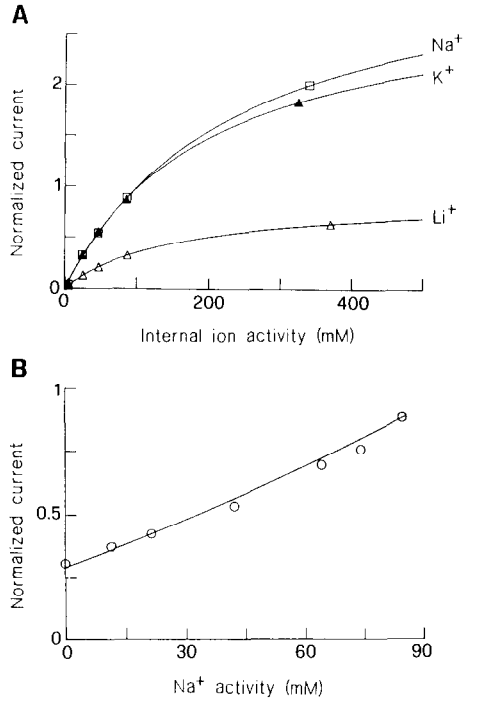

Fig. 6. (A) Dependence of the current activated by 100 μM cGMP in an excised patch from a retinal rod on the internal ion activity of Na, K or Li at +90 mV. Continuous lines were obtained from the Michaelis–Menten Eq. (3) with $K_{m,X}$ at +90 mV equal to 249, 203 and 160 mM for Na, K and Li respectively. (B) Currents measured as a function of the mole fraction of Na and Li at +90 mV. Reproduced from Ref. [28].

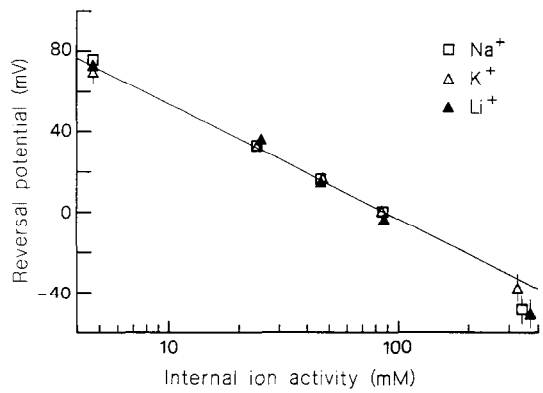

Fig. 5. Reversal potential of the current activated by 100 μM cGMP in a patch excised from a retinal rod as a function of internal ion activity for Na, Li or K. Continuous line was obtained from the GHK Eq. (2) with $P_X/P_{Na} = 1$. (□) Na^+, (△) K^+, (▲) Li^+. Reproduced from Ref. [28].

In order to characterize the ionic permeation through cyclic nucleotide activated channels the currents and the permeability ratios as a function of cation concentration were studied both in the retinal rod [28,32] and in the cone channel [20].

Currents through cGMP-gated channels in retinal rods were measured when the internal concentration of Na, K or Li was changed. Fig. 5 shows the reversal potentials plotted as a function of internal ion activity [28]. The continuous line is the theoretical reversal potential calculated from the Goldman–Hodgkin–Katz potential Eq. (2) and shows that the permeability ratios do not depend on the internal ion activity of Na, Li or K. The retinal cone channel also shows permeability ratios independent from ion activity for Na and Li (see Fig. 10 of Ref. [20]).

Fig. 6A shows the average steady-state current through cGMP-activated channels in retinal rods measured at +90 mV as a function of the internal activity of Na, K or Li. The current saturates as the ionic activity increases. The experimental data could be very well fitted by the Michaelis–Menten equation:

$$I_X = I_{max,X}[X]_i/([X]_i + K_{m,X}) \quad (3)$$

where I_X is the current carried by the ion X, $[X]_i$ is its activity at the intracellular side of the membrane patch, $I_{max,X}$ is the saturating current and $K_{m,X}$ is the half-saturating activity of the ion X. The values for $I_{max,X}$ and $K_{m,X}$ usually depend on the transmembrane potential. At +90 mV the value of K_m for the retinal rod channel was 249, 203 and 160 mM for Na, K and Li, respectively [28]. Similar experiments in the retinal cone channel gave the following values of K_m at +80 mV: 104 mM for Na and 37.6 mM for Li (see Fig. 9 in Ref. [20]). Therefore in both channels Li has a higher affinity for the channel than Na.

The current through retinal rod channels in solutions containing mixtures of Na and Li increased monotonically with Na activity, as shown in Fig. 6B. A similar result was also obtained in the olfactory channel (see Fig. 4 in Ref. [22]).

The described results obtained in retinal rods and cones, and in olfactory receptor cells are consistent with a model of cyclic nucleotide-gated channels as one-ion pores with a high-field-strength binding site. However, the analysis of inward Na conductances of cGMP-gated channels in retinal rods showed that they were reduced by the presence of some alkali and organic cations at the cytoplasmic side of the membrane (see Section 3.2 and Ref. [28,33]. This effect can be interpreted by assuming that the cGMP-gated channel of retinal rods, in addition to a narrow portion behaving as a one-ion pore, has a large vestibule at the cytoplasmic side with weakly voltage-dependent binding sites, which can be occupied by a permeating or a non-permeating ion.

3.2. Organic monovalent cations and pore size

Recent experiments have shown that at least 13 organic monovalent cations are permeable through the cGMP-gated channel from retinal rods, as summarized in Table 3 [33].

Table 3
Permeability ratios for organic cations in the cGMP-gated channel of retinal rods

Cation	P_X / P_{Na}
Hydroxylammonium	5.92
Ammonium	2.80
Hydrazinium	1.99
Methylhydroxylammonium	1.15
Guanidinium	1.12
Formamidinium	1.00
Aminoguanidinium	0.63
Methylammonium	0.60
Acetamidinium	0.36
Methylguanidinium	0.33
Ethanolammonium	0.19
Ethylammonium	0.16
Dimethylammonium	0.14

Permeability ratios relative to Na, P_X / P_{Na}, calculated with the GHK Eq. (2) for the cGMP-gated channel of retinal rod from the salamander [33].

Hydroxylammonium, hydrazinium and methylammonium, which are molecules of very similar shape, size and molecular weight, permeate the channel with very different permeability ratios relative to Na: 5.92, 1.99 and 0.6, respectively. These different permeabilities indicate that the cGMP-gated channel does not discriminate among ions on the basis of the cation dimensions only, but that chemical interactions are important in determining ion selectivity.

Guanidinium and some of its derivatives including aminoguanidinium and methylguanidinium are permeant, as shown in Figs. 7 and 8 and their permeability ratio relative to Na is 1.12, 0.63 and 0.33, respectively.

It was found that also some methylated and ethylated ammonium compounds are permeant, as shown in Table 3.

Eisenman et al. [30] studied the binding of five 'main species' organic cations to a site of different field strength and they generated a pattern of eleven possible selectivity sequences, analogous to those for alkali cations [34]. The experiments summarized in Table 3 show that the permeability sequence for the cGMP-activated channel for retinal rods is: ammonium > hydrazinium > guanidinium = formamidinium > aminoguanidinium, corresponding to sequence X predicted for a high-field-strength site. Therefore, the permeability sequences for alkali (see Section 3.1

and Table 2) and the 'main species' organic monovalent cations are in agreement with the prediction of the theory for a high-field-strength binding site.

By estimating the size of all permeant organic cations from space-filling models it is possible to obtain an estimate of the size of the narrowest region of the pore. The largest permeant ion is methylguanidinium, whose smallest dimensions are 0.38×0.59 nm. However, by taking into account the formation of hydrogen bonds within the channel, the effective dimensions could be reduced, and it is estimated that all permeant cations will fit in a pore of 0.38×0.5 nm dimensions [33].

3.3. Divalent cations

Cyclic nucleotide activated channels are also permeant to divalent cations and in physiological conditions they allow Ca to enter the cell. The permeability to divalent cations has been measured in intact cones [35], rods [36,37] and olfactory receptor cells [38,39] and indicates that a variety of divalent cations can permeate cyclic nucleotide-activated channels. Recently, the permeation properties of divalent cations have also been studied in excised patches from retinal rod outer segments [17]. With 110 mM NaCl at the extracellular side of the patch and only divalent cations present at equiosmolar concentrations (73.3 mM) at the intracellular side a small outward current carried by divalent cations and activated by 100 μM cGMP was measured [17]. The ratio of the outward current carried at +60 mV by the divalent cations analyzed and by Na over the current carried by Ca is:

$$Na:Sr:Ca:Ba:Mg:Mn = 83.3:1.4:1:0.58:0.33:0.25 \quad (4)$$

Divalent cations not only permeate but also block the cyclic nucleotide-activated channels as described in Sections 3.4 and 4.

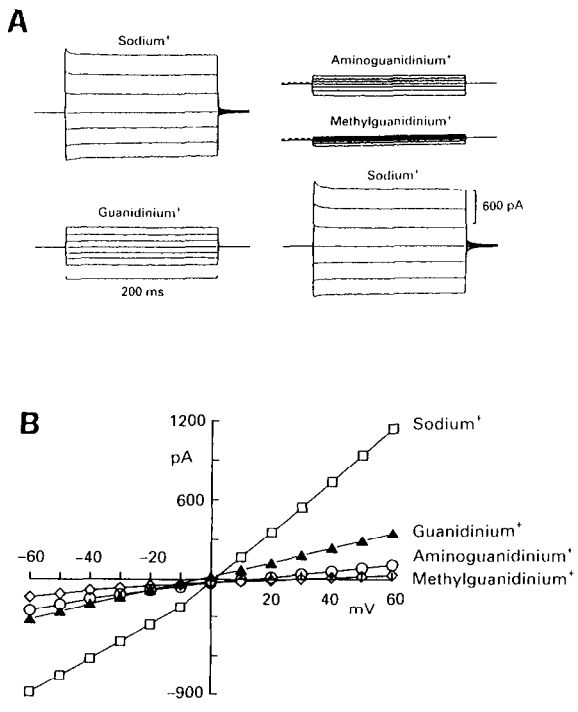

Fig. 7. (A) Currents activated by 100 μM cGMP in a patch excised from a retinal rod in the presence of guanidinium or its derivatives aminoguanidinium and methylguanidinium. (B) Current–voltage relations from the experiments shown in (A). Modified from Ref. [33].

3.4. Blockage by divalent cations and protons

Addition of millimolar concentrations of divalent cations to the cytoplasmic solution bathing an excised patch from retinal rod outer segment blocks the cGMP-gated current [17,32,40]. The blocking effect of divalent cations is voltage-dependent and the sequence of the blockage of the outward Na current activated by 100 μM cGMP at +60 mV is [17]:

$$Mg > Mn > Ba > Ca > Sr \quad (5)$$

The sequence (5) of the blocking potency of divalent cations is almost the reverse of their selectivity sequence (4), suggesting that the blocking potency by a divalent cation is inversely related to its ability to carry outward current. This observation together with the voltage-dependency of the blockage indicates that divalent cations block the cGMP-gated channel by entering it and occupying one [32] or more [40] binding sites for which cations compete in order to permeate.

Several factors are likely to contribute to the voltage-dependence of the blocking effect of divalent cations, indeed divalent cations can block the current by reducing the open probability and/or the single-channel conductance. Analysis of the blocking effect of Ca and Mg on single channels appears to be

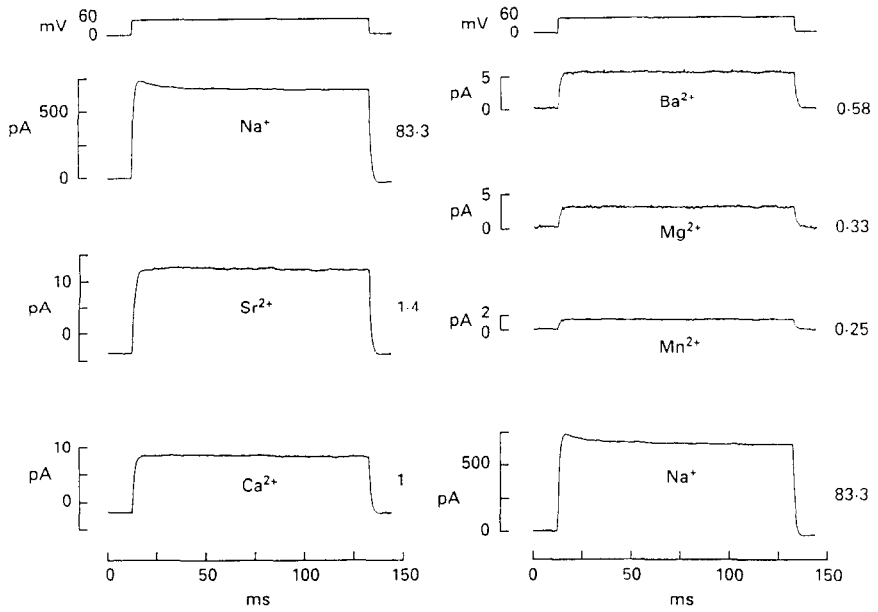

Fig. 8. Currents carried by divalent cations in a patch from a retinal rod. The medium bathing the cytoplasmic side of the membrane patch contained 110 mM NaCl or 73.3 mM of the chloride salt of divalent cations, as indicated in the figure. Numbers adjacent to each trace are the ratio of the current carried by each cation over the current carried by Ca. Currents were activated by 100 μM cGMP. Voltage steps were from 0 to +60 mV. Reproduced from Ref. [17].

different in the retinal rod and in the olfactory channel and it will be discussed in Section 5.1.

The effect of protons on cyclic nucleotide-gated channels was studied by changing the pH of the solution bathing the cytosolic side of inside-out patches from retinal rods [41,42] and from olfactory receptor cells [22]. When channels are activated by cGMP in retinal rods and by cAMP in olfactory receptor cells currents are blocked by lowering the pH of the cytoplasmic solution. Current inhibition is not voltage-dependent and has apparent pKs of 5.4 and 9.8 in retinal rods [41] and of 5.2 in olfactory receptor cells [22]. The absence of voltage dependence of proton blockage suggests that one or more titratable groups reside on the cytosolic face of the channel and not within the pore structure.

An interesting effect has been recently found in retinal rods analyzing the effect of pH when the visual channel is activated by cAMP instead of cGMP. As the bath pH is lowered the maximal current activated by cAMP increases whereas that activated by cGMP decreases, as described above. Moreover lowering the cytoplasmic pH causes a decrease of the $K_{1/2}$ (see Eq. 1) for cAMP whereas that for cGMP is unchanged. These results suggest that protons may affect the cyclic nucleotide activation of the channel either by changing the affinity for the binding site and/or the gating of the channel [18,27].

4. Single-channel properties

The first reports on single-channel properties of the retinal rod channel [14,43] indicated a single-channel conductance in the absence of divalent cations of 25 pS and a subconductance state of 8 pS with a mean open time ranging from 0.1 to 1 ms. However, recent studies [44] have shown the existence of two types of cGMP-gated channels from retinal rods: one type of channel is characterized by a rapid flickering between the open and closed state and the other type, rarely found, has well-resolved

transitions between the open and closed state. The rapid flickering is an intrinsic property of the first type of channel, is largely independent of membrane voltage [44], is not affected by the presence of cytoplasmic Ca or Mg [44] and is not significantly reduced by lowering the temperature from 24 to 8° C [45].

The flickering of the retinal rod channel in the absence of divalent cations is so rapid that the mean open time and the single-channel conductance cannot be directly measured but only indirectly estimated. The mean open time has been estimated to be no longer than the time constant of the recording system, about 35 μs, and the single-channel conductance at least 60 pS [44,45].

Torre and collaborators [44,45] have recently shown that, contrary to previous reports, single-channel activity can be seen in excised patches from retinal rods even in the presence of cytoplasmic millimolar amounts of Ca or Mg and they analyzed the blocking effect of Ca and Mg on single channels. Ca reduces the cGMP activated current of retinal rods by reducing the open probability and by decreasing the single-channel conductance. The reduction of the open probability caused by Ca is not voltage-dependent and is predominant in the presence of low concentrations of cGMP and at membrane potential more negative than -60 mV whereas the decrease of the single-channel conductance is voltage-dependent and is predominant at saturating cGMP concentrations. Mg ions block the current activated by cGMP in retinal rods in a different way: their blocking effect is more voltage dependent and they act reducing the single-channel conductance.

In the absence of divalent cations the substitution of Na at the cytoplasmic side of the patch with alkali monovalent cations does not alter the gating of the cGMP-gated channel of retinal rods [45,46]. Therefore the ionic selectivity obtained by measuring macroscopic currents (see Section 3.1) is similar to the selectivity determined at a single channel level.

The single-channel conductance of the retinal cone channel in the absence of divalent cations has different values depending on the animal species: 50 pS in the catfish [19], 14 pS in the carp [47], and 16 pS in the striped bass [48]. The unit conductance of the olfactory channel also depends on the animal species: values ranging from 21 to 55 pS have been reported [21,23,49,50]. Ca at the cytoplasmic side of excised patches from olfactory receptor cells of the salamander does not change the single-channel conductance but only reduces the open probability [51].

5. Structure

By cloning and sequencing of complementary DNA the primary structure of cyclic nucleotide-gated channels from retinal rods [52], cones [53] and olfactory receptor cells [54,55] have been determined. The deduced amino acid sequences show a high degree of similarity among these channels. The putative cyclic nucleotide binding site comprises 80–100 amino acid residues similar to the cyclic nucleotide binding domain of cGMP-dependent protein kinase. A site-specific mutagenesis study has shown that a threonine residue in this region (Thr-560 in the bovine rod channel and Thr-537 in the bovine olfactory channel) influences binding site specificity for cGMP over cAMP [56,57]. Little else is known about the mechanism of activation of the channel by cyclic nucleotides. A photoaffinity analog of cGMP has been recently developed for further studies of the cGMP-binding site [58].

Cyclic nucleotide-gated channels have many similarities with voltage-gated ion channels: an S_4 segment similar to the voltage sensor and a putative pore region P. The function of the S_4 region has not been identified while the P region forms an integral part of the ion conduction pore [59,60]. A glutamate residue (Glu-363) in the pore region of the retinal rod cloned channel represents a binding site for monovalent and divalent cations [61,62].

Besides these important findings on the structure of cyclic nucleotide-gated channels some properties of the cloned channels are different from those of the native channels. The cloned retinal rod channel has well-resolved single-channel openings [52,63] whereas the native channel is characterized by a continuous flickering between the open and closed state [44,45] as described in Section 4. Li is less permeant than Na in the cloned channel [52,60,62] whereas it is more permeant in the native channel [28]. Moreover the cloned channel is less sensitive to the blocking by l-cis-diltiazem than the native channel [52,57]. The cloned olfactory channel is much

less sensitive to cAMP [50,54,56] than the native channel [13,22,50]. Recently, additional subunits of the retinal rod [64] and the olfactory [65,66] channel have been identified. These protein do not form functional channels by themselves but only when co-expressed with the previously cloned channel protein. The retinal rod channel composed by the two subunits is more similar to the native channel in the rapid flickering of single channels and in the sensitivity to blockage by l-cis-diltiazem [64]. The olfactory channel composed by the two subunits has an increased sensitivity to cAMP, near that of the native channel [65,66]. Therefore the native cyclic nucleotide-gated channels seem to be hetero-oligomers composed by at least two different types of subunits.

6. Other channels gated by cyclic nucleotides

Channels gated by cyclic nucleotides not only mediate sensory transduction in vertebrate olfactory receptor and photoreceptor cells, but they are also present in other cells. Among others, they are found in cells of the pineal gland [67], retinal bipolar cells [68,69], retinal ganglion cells [70] and in sperm [71].

Acknowledgements

This work was supported by the European Community Grant BRA SSS 6961. I thank V. Torre for comments on the manuscript, Ms. L. Giovanelli for checking the English and Ms. M. Zanini for help in preparing the figures.

References

[1] S. Forti, A. Menini, G. Rispoli and V. Torre, J. Physiol., 419 (1989) 265.
[2] S. Firestein, C. Picco and A. Menini, J. Physiol., 468 (1993) 1.
[3] T.D. Lamb and E.N. Pugh, TINS, 15 (1992) 291.
[4] P.A. McNaughton, Physiol. Rev., 70 (1990) 847.
[5] E.N. Pugh and T.D. Lamb, Vision Res., 30 (1990) 1923.
[6] U.B. Kaupp and K.W. Koch, Annu. Rev. Physiol., 54 (1992) 153.
[7] R.R. Reed, Neuron, 8 (1992) 205
[8] G.M. Shepherd, in D.P. Corey and S.D. Roper (Editors), Sensory Transduction, The Rockefeller University Press, New York, 1992, p. 20.
[9] T.D. Lamb and E.N. Pugh, J. Physiol., 449 (1992) 719.
[10] D. Tranchina, J. Sneyd and I.D. Cadenas, Biophys. J., 60 (1991) 217.
[11] E.E. Fesenko, S.S. Kolesnikov and A.L. Lyubarski, Nature, 313 (1985) 310.
[12] L.W. Haynes and K.W. Yau, Nature, 317 (1985) 61.
[13] T. Nakamura and G.H. Gold, Nature, 325 (1987) 442.
[14] A.L. Zimmerman and D.A. Baylor, Nature, 321 (1986) 70.
[15] J.C. Tanaka, J.F. Eccleston and R.E. Furman, Biochemistry, 28 (1989) 2776.
[16] H. Luhering, W. Hanke, R. Simmoteit and U.B. Kaupp, in A. Borsellino, L. Cervetto and V. Torre (Editors), Sensory Transduction, Plenum Press, New York, 1990, p. 169.
[17] G. Colamartino, A. Menini and V. Torre, J. Physiol., 440 (1991) 189.
[18] A. Menini, C. Sanfilippo and C. Picco, Proc. XXXII Congress IUPS, 1993, p. 168.
[19] L.W. Haynes and K.W. Yau, J. Physiol., 429 (1990) 451.
[20] A. Picones and J.I. Korenbrot, J. Gen. Physiol., 100 (1992) 647.
[21] F. Zufall, S. Firestein and G.M. Shepherd, J. Neurosci., 11 (1991) 3573.
[22] S. Frings, Y.W. Lynch and B. Lindemann, J. Gen. Physiol., 100 (1992) 45.
[23] T. Kurahashi and A. Kaneko, J. Physiol., 466 (1993) 287.
[24] S.E. Gordon, D.L. Brautigan and A.L. Zimmerman, Neuron, 9 (1992) 739.
[25] Y.T. Hsu and R.S. Molday, Nature, 361 (1993) 76.
[26] T.Y. Chen and K.W. Yau, Nature, 368 (1994) 545.
[27] C. Sanfilippo and A. Menini, Biophys. J., 64 (1993) A17.
[28] A. Menini, J. Physiol., 424 (1990) 167.
[29] R.E. Furman and J.C. Tanaka, J. Gen. Physiol., 96 (1990) 57.
[30] G. Eisenman and R. Horn, J. Membrane Biol., 76 (1983) 197.
[31] B. Hille, Ionic Channels of Excitable Membranes, Sinauer Ass., Sunderland, 1992.
[32] A.L. Zimmerman and D.A. Baylor, J. Physiol., 449 (1992) 759.
[33] C. Picco and A. Menini, J. Physiol., 460 (1993) 741.
[34] G. Eisenman, S. Krasne and S. Ciani, in Kessler et al. (Editors), Ion Selective Electrodes and Enzyme Electrodes in Medicine and Biology, Urban and Schwarzenberg, Munich, 1976, p. 3.
[35] R.J. Perry and P.A. McNaughton, J. Physiol., 433 (1991) 561.
[36] A.L. Hodgkin, P.A. McNaughton and B.J. Nunn, J. Physiol., 358 (1985) 447.
[37] A. Menini, G. Rispoli and V. Torre, J. Physiol., 402 (1988) 279.
[38] T. Kurahashi and T. Shibuya, Brain Res., 515 (1990) 261.
[39] S. Frings, S. Benz and B. Lindemann, J. Gen. Physiol., 97 (1991) 725.
[40] J.C. Tanaka and R.C. Furman, J. Membrane Biol., 131 (1993) 245

[41] A. Menini and B.J. Nunn, in A. Borsellino, L. Cervetto and V. Torre (Editors), Sensory Transduction, Plenum Press, New York, 1990, p. 175.
[42] J.C. Tanaka, Biophys. J., 65 (1993) 2517.
[43] L.W. Haynes, A.R. Kay and K.W. Yau, Nature, 321 (1986) 66.
[44] V. Torre, M. Straforini, F. Sesti and T.D. Lamb, Proc. R. Soc. London B, 250 (1992) 209.
[45] F. Sesti, M. Straforini, T.D. Lamb and V. Torre, J. Physiol., 474.2 (1994) 203.
[46] A. Menini, C. Picco, E. DeMicheli and F. Conti, Biophys. J., 59 (1991) 535a.
[47] S.I. Watanabe and M. Murakami, Visual Neurosci., 6 (1991) 563.
[48] A. Picones and J.I. Korenbrot, Biophys. J., 66 (1994) 360.
[49] N. Suzuki, Neurosci. Res. Suppl., 12 (1990) S113.
[50] E.H. Goulding, J. Ngai, R.H. Kramer, S. Colicos, R. Axel, S.A. Siegelbaum and A. Chess, Neuron, 8 (1992) 45.
[51] F. Zufall, G.M. Shepherd and S. Firestein, Proc. R. Soc. London B, 246 (1991) 225.
[52] U.B. Kaupp, T. Niidome, T. Tanabe, S. Terada, W. Boenigk, W. Stuehmer, N.J. Cook, K. Kangawa, H. Matsuo, T. Hirose, T. Miyata and S. Numa, Nature, 342 (1989) 762.
[53] W. Bonigk, W. Altenhofen, F. Muller, A. Dose, M. Illing, R.S. Molday and U.B. Kaupp, Neuron, 10 (1993) 865.
[54] R.S. Dhallan, K.W. Yau, K.A. Schrader and R.R. Reed, Nature, 347 (1990) 184.
[55] J. Ludwig, T. Margalit, E. Eismann, D. Lancet and U.B. Kaupp, FEBS Lett., 270 (1990) 24.
[56] W. Altenhofen, J. Ludwig, E. Eismann, W. Kraus, W. Boenigk and U.B. Kaupp, Proc. Natl. Acad. Sci. USA, 88 (1991) 9868.
[57] U.B. Kaupp, Trends Neurosci., 14 (1991) 154.
[58] R.L. Brown, W.V. Gerber and J.W. Karpen, Proc. Natl. Acad. Sci USA, 90 (1993) 5369.
[59] L. Heginbotham, T. Abramson and R. MacKinnon, Science, 258 (1992) 1152.
[60] E.H. Goulding, G.R. Tibbs, D. Liu and S.A. Siegelbaum, Nature, 364 (1993) 61.
[61] M.J. Root and R. MacKinnon, Neuron, 11 (1993) 459.
[62] E. Eismann, F. Muller, S.H. Heinemann and U.B. Kaupp, Proc. Natl. Acad. Sci. USA, 91 (1994) 1109.
[63] M. Nizzari, F. Sesti, M.T. Giraudo, C. Virginio, A. Cattaneo and V. Torre, Proc. R. Soc. London B, 254 (1993) 69.
[64] T.Y. Chen, Y.W. Peng, R.S. Dhallan, B. Ahamed, R.R. Reed and K.W. Yau, Nature, 362 (1993) 764.
[65] E. Liman and L. Buck, Neuron, (1994).
[66] J. Bradley, J. Li, N. Davidson, H.A. Lester and K. Zinn, Proc. Natl. Acad. Sci. USA, 91 (1994) 8890.
[67] S.E. Dryer and D.A. Henderson, Nature, 353 (1991) 756.
[68] S. Nawy and C.E. Jahr, Nature, 346 (1990) 269.
[69] R.A. Shiells and G. Falk, Proc. R. Soc. London B, 242 (1990) 91.
[70] I. Ahmad, T. Leinders-Zufall, J.D. Kocsis, G.M. Shepherd, F. Zufall and C.J. Barnstable, Neuron, 12 (1994) 155.
[71] I. Weyand, M. Godde, S. Frings, J. Weiner, F. Muller, W. Altenhofen, H. Hatt and U.B. Kaupp, Nature, 368 (1994) 859.